


RESEARCH ARTICLE

Associations between femoral 3D curvature and sagittal imbalance of spine

Chien-Hsiung Lo¹ | Yu-Hua Dean Fang^{2,3} | Jing-Yao Wang³ | Tzu-Ping Yu¹ |
Hao-Chun Chuang¹ | Yuan-Fu Liu¹ | Chao-Jui Chang^{1,4} | Cheng-Li Lin^{1,3,5,6} 

¹Department of Orthopedic Surgery, National Cheng Kung University Hospital, College of Medicine, National Cheng Kung University, Tainan, Taiwan

²Department of Radiology, School of Medicine, University of Alabama at Birmingham, Birmingham, Alabama, USA

³Department of Biomedical Engineering, College of Engineering, National Cheng Kung University, Tainan, Taiwan

⁴Department of Orthopaedics, Dou-Liou Branch of National Cheng Kung University Hospital, Yunlin, Taiwan

⁵Musculoskeletal Research Center, Innovation Headquarter, National Cheng Kung University, Tainan, Taiwan

⁶Medical Device Innovation Center, National Cheng Kung University Hospital, Tainan, Taiwan

Correspondence

Cheng-Li Lin, Department of Orthopaedics, National Cheng Kung University Hospital, No. 138, Sheng-Li Road, Tainan City, 70428, Taiwan.
Email: jengli94@gmail.com

Funding information

Ministry of Science and Technology, Taiwan, Grant/Award Numbers: MOST 108-2813-C-006-114-B, MOST 110-2314-B-006 -027 -MY3; National Cheng Kung University, Grant/Award Number: NCKUMCS2019040; National Cheng Kung University Hospital, Grant/Award Number: NCKUH-11202056

Abstract

Background: The sagittal imbalance (SI) of spine triggers compensatory mechanisms (CMs) of lower extremity (LE) to restore trunk balance. These CMs can cause long-period stress on the femur and may possibly alter the femoral morphology. This cross-sectional observational study aimed to answer the following questions: (a) Do SI subjects exhibit greater femoral bowing compared to subjects with sagittal balance? (b) Are there associations between femoral bowing and CMs of LE in SI subjects?

Methods: Subjects who underwent biplanar full body radiographs with the EOS imaging system between January 2016 and September 2021 were recruited. Sagittal parameters included T1-pelvic angle (TPA), pelvic incidence (PI), pelvic tilt (PT), sacral slope, lumbar lordosis (LL), PI-LL, and PT/PI ratio. LE parameters were femoral obliquity angle (FOA), knee flexion angle (KA), and ankle dorsiflexion angle. Femoral bowing was quantified as 3D radius of femoral curvature (RFC). Associations between 3D RFC and the radiographic parameters were analyzed.

Results: A total of 105 subjects were included, classified into balance group (TPA < 14°, *n* = 40), SI group (TPA ≥ 14° and KA < 5°, *n* = 30), and SI with knee flexion group (TPA ≥ 14° and KA ≥ 5°, *n* = 35). 3D RFC was significantly lower in SI with knee flexion group compared to the other two groups (both *p* < 0.001). Stepwise linear regression showed that age, SI and knee flexion, femoral length (FL), FOA, and KA were independent predictors for 3D RFC.

Conclusion: Greater femoral bowing is observed in subjects with SI and knee flexion compared to the balanced population. CM parameters, including KA and FOA, are associated with 3D RFC. Further longitudinal study is needed to investigate the cause-and-effect relationship between SI, CMs of LE, and femoral bowing.

KEYWORDS

EOS, femoral bowing, knee flexion angle, sagittal imbalance

1 | INTRODUCTION

Spine sagittal imbalance (SI) refers to a clinical condition caused by sagittal spinopelvic malalignment with which the patients exhibit forward leaning trunk and anteriorly shifted gravity line. The malalignment can be resulted from iatrogenic causes, spinal pathology, or aging process. To effortlessly maintain an upright posture and a horizontal gaze, multiple compensatory mechanisms (CMs) from different levels including spine, pelvis, and lower extremities (LE) are recruited progressively.¹⁻³ The CMs of LE such as hip extension, knee flexion, and ankle extension have been demonstrated to help restore trunk balance.⁴

Femoral bowing has long been a stressed topic studied by radiologists and orthopedic surgeons because of its wide clinical applications such as design of orthopedic implants (e.g., total knee arthroplasty, plate, and intramedullary nail for fixation) and prevention of surgical complications. The quantification methods and correlated variables vary between related studies, of which femoral length and age are the predictive factors.^{5,6} Nevertheless, the correlation between the SI and femoral bowing has not been studied yet. To investigate the lower limb alignment and morphology, particularly the femoral bowing of SI population, a radiographic evaluation of whole spine and full-length lower limb alignment is required. The EOS imaging system is a well-validated clinical imaging tool featured with low radiation doses⁷ (50%–80% less than conventional X-rays⁸) and capability of simultaneous acquisition of high-quality full body image in both sagittal and coronal planes. It also concurrently provides spinopelvic parameters and the low extremity alignment under physiological weight-bearing conditions similar to the status of daily life.

The interindividual differences in cumulative stress on femur over time may lead to wide variations in a certain femoral morphology.⁹ The objective of the present study is to investigate the association between SI, CMs, and 3D radius of femoral curvature (RFC) via EOS imaging system.

2 | MATERIALS AND METHODS

2.1 | Ethical review committee statement

This is a retrospective study using data and images obtained for clinical purposes. We consulted extensively with the Institutional Review Board (IRB) of National Cheng Kung University Hospital for the determination that our investigation did not need ethical approval or informed consent. An IRB official waiver of ethical approval was granted from the IRB of National Cheng Kung University Hospital (No. B-ER-106-210).

2.2 | Study population

This retrospective, cross-sectional study reviewed subjects who underwent biplanar full body radiographs with the EOS imaging system at a single medical center between January 2016 and September

2021. Inclusion criteria were: (a) age >50 and (b) patients with full body stereo-radiograph (EOS Imaging SA., Paris, France) due to clinical suspicion of degenerative spine diseases or spinal deformity. Exclusion criteria were: (a) history of femoral fracture, spinal surgery, and operation involving femoral implants such as total hip arthroplasty (THA), total knee arthroplasty (TKA), or intramedullary nailing and (b) poor image quality due to motion artifact or overpenetration. Demographics data including age, sex, and BMI were collected.

2.3 | Images

The EOS imaging system, a slot-scanning radiograph imager, allowed the acquisition of whole-body radiograph images while the subjects were in a weight-bearing position. During the scan, subjects were asked to maintain a standardized free standing position with the shoulder and elbow anteriorly flexed and hands rested on the mandibles and a shifted feet position, as proposed by Chaibi et al.¹⁰ This allowed the examination of the spine and lower limbs under normal weight-bearing conditions. In addition, true-to-size images were obtained as the system employed the detection of two orthogonally co-linked and collimated linear X-ray beam.^{11,12}

2.4 | Radiographic parameters

All parameters were measured and calculated in the anatomogravitational frame^{13,14} by senior radiologists or orthopedists using the “sterEOS” software bundled with the EOS imaging system. The measured radiographic parameters are specified as follows (Figure 1):

2.4.1 | Spinopelvic

- C7-Sagittal vertical axis (C7-SVA): the horizontal offset between the posterosuperior corner of S1 and the plumb line of C7, the vertical line through the center of the C7 vertebral body. A greater value represents a higher severity of SI.²
- T1 pelvic angle (TPA): this corresponds to the angle between a line connecting the center of T1 to the center of the femoral heads (CFH) and a line from the CFH to the center of the S1 endplate. Subjects were classified into sagittal balance and imbalance group on the basis of their TPA values (<14° or ≥14°).¹⁵ A greater value signifies a more severe SI.¹⁵
- Lumbar lordosis (LL): the angle between the superior L1 and sacral endplates.
- Pelvic incidence (PI): the angle between a line perpendicular to the sacral plate and the line connecting the midpoint of the sacral plate to the CFH.^{11,16}
- Pelvic tilt (PT): the angle between a vertical line and the line connecting the midpoint of the sacral plate to the CFH.^{11,16}
- Sacral slope (SS): the angle between the horizontal line and the sacral plate.¹⁶



FIGURE 1 Demonstrations of the measured radiographic sagittal parameters. FOA, femoral obliquity angle; KA, knee flexion angle; PI, pelvic incidence; PT, pelvic tilt; SS, sacral slope; SVA, sagittal vertical axis; TPA, T1-pelvic angle.

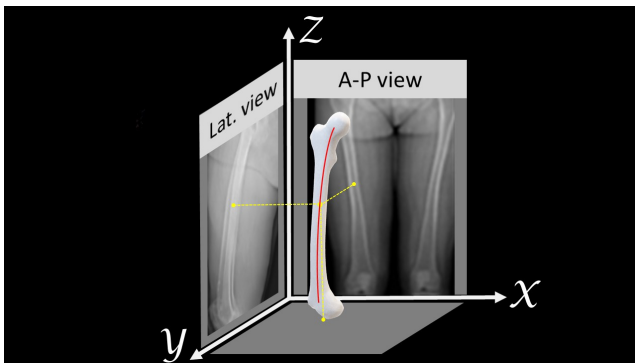


FIGURE 2 An imaginary spatial coordinate system, with yellow dots representing the projected points of the femur at specific locations in three-dimensional space onto sagittal plane (lateral view) and coronal plane (anterior-posterior [A-P] view). The red curve signifies the hypothetical curve passing through the central axis of the femoral medullary canal in three-dimensional space. As demonstrated, the x and z coordinates can be obtained from the A-P view, and the y and z coordinates from the lateral view. Using the z coordinate as benchmark and combining the two plane coordinates obtained from each view, the spatial coordinate (x,y,z) of a specific point of femur can be obtained.

- PI-LL: the mismatch between PI and LL, indicating a degree of loss of lordosis.
- PT/PI: indicating a degree of pelvic compensation in sagittal imbalanced subjects.

2.4.2 | Lower extremities

- Femoral obliquity angle (FOA), also known as proximal femoral angle: the angle between the femoral axis and the vertical line, representing the obliquity of femur on lateral view.
- Knee flexion angle (KA): the angle between the mechanical axis of the femur and that of the tibia.²

- Ankle dorsi-flexion angle (AA): The mean angle of bilateral ankle flexion angles between the line from the midpoint of bilateral femoral condylar notches to the midpoint of distal tibial joint surfaces and the vertical line from the midpoint of distal tibial joint surfaces.¹⁷

2.5 | Radiographic radius of femoral curvature¹⁸

Coordinates were obtained using the sterEOS “software bundled with the EOS” imaging system.

2.5.1 | “Construction of femur-specific spatial coordinate system” (Figure 2)

1. Draw two horizontal lines passing through the lower edge of lesser trochanter¹⁹ and the upper edge of medial epicondyle, respectively, to define the proximal and distal end of the femoral shaft on the anteroposterior view. As illustrated, the distal end represents the X-Y plane of the system.
2. Draw a vertical line connecting the two ends of the femoral shaft, which represents the Z-axis.
3. Mark the $\frac{1}{2}$ point, lower $\frac{1}{4}$ point, and upper $\frac{1}{4}$ point on the Z-axis, correspondingly demonstrating the mid-points of proximal third, middle third, and distal third of femur.
4. Mark two additional points on the Z-axis, one at 5 cm above the upper $\frac{1}{4}$ point and the other at 5 cm below the lower $\frac{1}{4}$ point.
5. Measure the horizontal distance from these anchor points to the center points of whole femur and femoral canal, respectively, on both views. The measurement displays the X-value on AP view and the Y-value on lateral view of the center points.
6. Measure the vertical distance from the anchor points to the distal end, indicating the Z-value of the center points.

7. The spatial coordinates (x,y,z) of the most proximal, middle, and distal center points were obtained by means of the aforementioned steps.

The accuracy and reliability of the measurement of spinopelvic parameters using sterEOS system have been reported.²⁰⁻²²

2.5.2 | 3D Radius of femoral curvature calculation

The 3D radius of femoral curvature (RFC) of the whole femur was mathematically calculated using the following formula:

1. Assume three non-collinear points $A(x_1,y_1,z_1)$, $B(x_2,y_2,z_2)$, $C(x_3,y_3,z_3)$ and the center of circumcircle of the triangle formed by such the three points (x_0,y_0,z_0) .
2. Solve the following simultaneous equations and calculate the 3D RFC:

$$\begin{cases} (x_0 - x_1)^2 + (y_0 - y_1)^2 + (z_0 - z_1)^2 = (x_0 - x_2)^2 + (y_0 - y_2)^2 + (z_0 - z_2)^2 \\ (x_0 - x_1)^2 + (y_0 - y_1)^2 + (z_0 - z_1)^2 = (x_0 - x_3)^2 + (y_0 - y_3)^2 + (z_0 - z_3)^2 \end{cases}$$

$$\begin{matrix} x_0 & y_0 & z_0 & 1 \\ x_1 & y_1 & z_1 & 1 \\ x_2 & y_2 & z_2 & 1 \\ x_3 & y_3 & z_3 & 1 \end{matrix} = 0$$

$$3D\text{ RFC} = \sqrt{(x_0 - x_1)^2 + (y_0 - y_1)^2 + (z_0 - z_1)^2}$$

3. The present study programmed a 3D RFC calculator based on above equation, which automatically output the 3D RFC after inputting spatial coordinates of three specific points.

Cortical RFC (CRFC) represents the 3D RFC of the whole femoral centerline, while medullary RFC (MRFC) describes the 3D RFC of the femoral canal centerline.

2.6 | Reliability and power analysis

Intra- and interobserver's reliabilities of the 3D RFC measurement were assessed by intraclass correlation coefficient (ICC).²³ An ICC of >0.75 was considered indicative of excellent agreement. The test-retest reliability of the 3D RFC measurement showed good to excellent agreement with an interobserver ICC of 0.865 (95% CI: 0.650–0.952) and an intra-observer ICC of 0.920 (95% CI: 0.808–0.974). A statistical power analysis was performed to estimate the sample size in each statistical results with G-power software.²⁴ On the basis of data from pivot study, the effect size (ES) was 0.7 in the independent t test and 0.56 in multiple regression analysis, respectively. With an alpha of 0.05 and power of 0.80, the estimated sample sizes required with such the ES were 56 for independent t test and 24 for multiple regression analysis. Therefore, the total sample size ($N = 105$) was more adequate for the main objective of this study.

2.7 | Statistical analysis

Quantitative variables are presented as r and analyzed by Pearson correlation. Binary variables with normal distribution are presented as

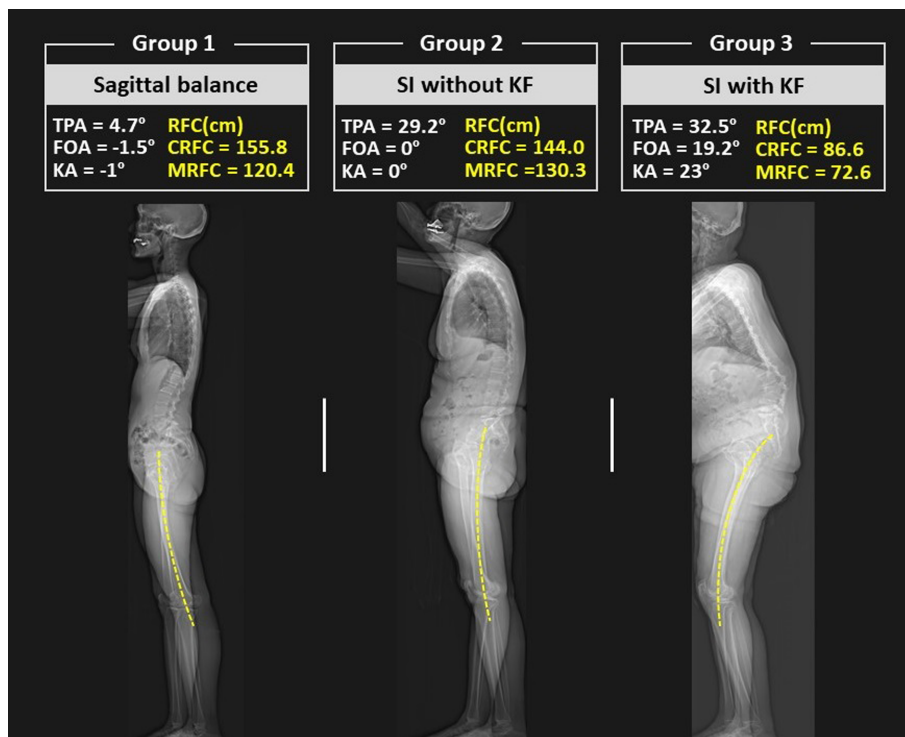


FIGURE 3 Sagittal full-body images, sagittal profiles, and 3D RFC of subjects from each subgroup. Greater femoral bowing can be visually observed from the image of the patient from group 3, compared to the other two subgroups, which is compatible with the results of measurement. KF, knee flexion; SI, sagittal imbalance.

mean \pm standard deviation (SD) and analyzed by using independent Student's *t* test, otherwise variables without normal distribution were presented as median (min.–max.) and analyzed by using Wilcoxon rank sum test. Two-tail *p*-value <0.05 were considered significant. Collinearity was assessed by Pearson correlation before multivariate linear regression modeling. A correlation coefficient of more than 0.75 were regarded as collinearity. In the case of collinearity, the most clinically relevant factors were kept in the model. In model 1, sagittal group, gender, age, BMI, FL, C7-SVA, PI-LL, SS, FOA, and AA were included into the stepwise procedure to select the final related parameters. In model 2, gender, age, BMI, FL, C7-SVA, TPA, SS, PT, KA, and AA were included into the stepwise procedure to select the final related parameters. Data above were analyzed using SPSS version 22.0 (IBM Corp. in Armonk, NY, USA).

3 | RESULTS

A total of 105 subjects were included in the study and classified into three groups. Definitions of each group are as follows, group 1 (balance group: TPA $< 14^\circ$, $n = 40$), group 2 (SI group: TPA $\geq 14^\circ$ and KA $< 5^\circ$, $n = 30$), and group 3 (SI and knee flexion group: TPA $\geq 14^\circ$ and KA $\geq 5^\circ$, $n = 35$) (Figure 3). Demographics, sagittal radiographic parameters, and 3D RFC of the study population are presented in Table 1. Subjects' mean \pm SD age was 68.7 ± 8.3 years and most were female (72.4%). The calculated 3D MRFC and CRFC of the whole femur were 110.2 ± 31.9 cm and 129.8 ± 42.9 cm, respectively.

The association between 3D RFC and study parameters is listed in Table 2. When adopting the TPA and KA definition for grouping, both MRFC and CRFC of sagittal group 1 and sagittal group 2 were considerably greater than sagittal group 3 ($p < 0.001$). In the univariate analysis, both MRFC and CRFC were moderately correlated with age ($r = -0.519$ and -0.511 , respectively), height ($r = 0.340$ and 0.339 , respectively), TPA ($r = -0.317$ and -0.347 , respectively), FOA ($r = -0.540$ and -0.559 , respectively), KA ($r = -0.528$ and -0.538 , respectively), and AA ($r = -0.349$ and -0.342 , respectively) (all $p < 0.001$). Moreover, weak correlations were revealed between 3D RFC and other variables including height, FL, C7-SVA, LL, PI-LL, SS, PT, and PT/PI.

We further conducted a stepwise method to select the independent predictive factors for the multivariate linear regression analysis (Table 3). Spearman correlation analysis was performed to assess the collinearity among the demographic covariates and sagittal parameters. Correlation coefficients higher than 0.75 were considered as indicators of collinearity (see Table S1). Based on the correlation analysis, sagittal group, gender, age, BMI, FL, C7-SVA, PI-LL, SS, FOA, and AA were included in model 1, while model 2 included gender, age, BMI, FL, C7-SVA, TPA, SS, PT, KA, and AA (Table 2). After applying the stepwise method, the sagittal group, FL, and FOA were selected as the correlated factors in model 1; and age, FL, and KA in model 2 (Table 3). Model 1 disclosed that FL was positively correlated to MRFC ($\beta = 0.295$, $p < 0.001$), group 3 (compared with group 1) and FOA was negatively correlated to MRFC

TABLE 1 Demographics, sagittal radiographic parameters, and 3D RFC of the 105 studied subjects.

Parameters	Mean	SD	Min.	Max.
Demographics				
Gender, n (M:F)	29:76			
Age (years)	68.7	8.3	50.0	90.0
Height (cm)	156.5	7.8	139.0	176.0
Weight (kg)	59.3	12.1	37.0	99.0
BMI (kg/m ²)	24.1	4.1	17.3	37.3
FL (cm)	38.4	2.0	34.5	44.0
Sagittal parameters				
C7-SVA (mm)	44.3	38.2	-22.0	171.0
TPA (°)	19.1	11.6	-0.8	61.7
LL (°)	37.0	18.7	-37.0	72.0
PI (°)	49.0	10.4	28.0	79.1
PI-LL (°)	12.4	17.7	-18.0	66.6
SS (°)	29.1	10.7	-11.0	51.0
PT (°)	19.9	10.8	1.6	52.0
PT/PI	0.4	0.2	0.1	1.3
FOA (°)	8.5	5.4	-2.3	23.0
KA (°)	4.4	6.1	-7.0	23.0
AA (°)	4.8	4.2	-2.3	18.2
3D RFC (cm)				
Medullary	110.2	31.9	57.2	213.9
Cortical	129.8	42.9	55.9	250.8

Abbreviations: AA, ankle dorsiflexion angle; BMI, body mass index; C7-SVA, C7-sagittal vertical axis; FL, femoral length; FOA, femoral obliquity angle; KA, knee flexion angle; LL, lumbar lordosis; PI, pelvic incidence; PT, pelvic tilt; RFC, radius of femoral curvature; SD, standard deviation; SS, sacral slope; TPA, T1-pelvic angle.

($\beta = -0.353$, $p = 0.002$; $\beta = -0.328$, $p = 0.003$, respectively). FL was positively correlated to CRFC ($\beta = 0.295$, $p < 0.001$), group 3 (compared with group 1) and FOA was negatively correlated to CRFC ($\beta = -0.461$, $p < 0.001$; $\beta = -0.213$, $p = 0.047$, respectively). These variables explained 38% of the variability in MRFC ($p < 0.001$, adjusted $R^2 = 0.383$) and 38% of the variability in CRFC ($p < 0.001$, adjusted $R^2 = 0.384$). In model 2, FL was positively correlated to MRFC ($\beta = 0.228$, $p = 0.005$), age and KA were negatively correlated to MRFC ($\beta = -0.274$, $p = 0.003$; $\beta = -0.386$, $p < 0.001$, respectively). FL was positively correlated to CRFC ($\beta = 0.227$, $p = 0.007$), age and KA were negatively correlated to CRFC ($\beta = -0.252$, $p = 0.008$; $\beta = -0.358$, $p < 0.001$, respectively). These variables explained 35% of the variability in MRFC ($p < 0.001$, adjusted $R^2 = 0.354$) and 31% of the variability in CRFC ($p < 0.001$, adjusted $R^2 = 0.306$). The comparison of variables among three groups is presented in Figure 4. No statistically significant difference was observed in RFC, age, TPA, and PI-LL between group 1 and 2, while significantly higher femoral bowing, age, TPA, and PI-LL were found between group 1 and group 3 or between group 2 and 3 (all $p < 0.001$).

TABLE 2 The association of 3D RFC, sagittal group, and parameters.

Variables	MRFC (cm)		CRFC (cm)	
	Mean ± SD or median (min.–max.) or <i>r</i>	<i>p</i>	Mean ± SD or median (min.–max.) or <i>r</i>	<i>p</i>
Group				
1: TPA < 14° (n = 40)	122.8 ± 36.0	<0.001	147.6 ± 45.3	<0.001
2: TPA ≥ 14° and KA < 5° (n = 30)	120.7 ± 24.4		144.6 ± 37.0	
3: TPA ≥ 14° and KA ≥ 5° (n = 35)	87.0 ± 16.5		96.7 ± 20.1	
Demographic information				
Gender				
Male (n = 29)	109.0 (69.0–212.4)	0.552	118.1 (74.0–250.3)	0.725
Female (n = 76)	102.2 (57.2–213.9)		119.2 (55.9–250.8)	
Age (years)	–0.519	<0.001	–0.511	<0.001
Height (cm)	0.340	<0.001	0.339	<0.001
Weight (kg)	0.058	0.555	0.069	<0.001
BMI (kg/m ²)	–0.110	0.262	–0.110	0.486
FL (cm)	0.204	0.037	0.196	0.263
Sagittal parameters				
C7-SVA (mm)	–0.241	0.013	–0.287	0.003
TPA (°)	–0.317	0.001	–0.347	<0.001
LL (°)	0.226	0.021	0.276	0.005
PI (°)	0.056	0.571	0.033	0.741
PI-LL (°)	–0.210	0.032	–0.277	0.004
SS (°)	0.298	0.002	0.327	0.001
PT (°)	–0.213	0.029	–0.265	0.006
PT/PI	–0.273	0.005	–0.323	0.001
Lower extremities				
FOA (°)	–0.540	<0.001	–0.559	<0.001
KA (°)	–0.528	<0.001	–0.538	<0.001
AA (°)	–0.349	<0.001	–0.342	<0.001

Note: *p*-value < 0.05 were consider significant.

Abbreviations: AA, ankle dorsiflexion angle; BMI, body mass index; C7-SVA, C7-sagittal vertical axis; CRFC, cortical radius of femoral curvature; FL, femoral length; FOA, femoral obliquity angle; KA, knee flexion angle; LL, lumbar lordosis; MRFC, medullary radius of femoral curvature; PI, pelvic incidence; PT, pelvic tilt; *r*, Spearman correlation coefficient; SD, standard deviation; TPA, T1-pelvic angle.

4 | DISCUSSION

The present study demonstrates that significantly greater femoral bowing is observed in subjects with SI and knee flexion compared to subjects with sagittal balance or with SI without knee flexion. Regression analysis reveals that femoral bowing is positively associated with age, SI and knee flexion, FOA, and KA, while inversely associated with FL. These findings suggest that in addition to age and FL, LE CMs in response to SI also play significant roles in determining femoral curvature. This highlights the complex interplay between SI, LE CMs, and femoral morphology, indicating that factors related to lower extremity alignment and balance can contribute to changes in femoral curvature.

Human femur is grossly depicted as having an anterior convexity,²⁵ and the quantification of femoral curvature has long been introduced and studied owing to its direct application in

designing femoral implants (e.g., TKA, THA, and intramedullary nails).^{26,27} Surgical complications led by uncompensated mismatches between the curve of the implants and the femur have been reported, including but not limited to iatrogenic fractures, cortical penetration, and cortical encroachment.^{28–30} However, the measurement methodology and the image modalities varied between previous studies. Most researchers conducted 2D RFC measurement on single AP or lateral radiograph; the concept and measurement of 3D RFC based on computer tomography have been introduced by Chantarapanich et al. and other investigators.^{6,18,25,31} In the present study, an innovative method utilizing the EOS imaging system to measure 3D RFC was proposed with reliable and reproductive results. The mean values of 3D RFC of our 105 Taiwanese participants (CRFC: 1295 mm; MRFC: 1101 mm) were similar to previously reported values from Asian populations (771–1240 mm).^{5,6,25,31}

TABLE 3 Multivariate stepwise linear regression analysis for the identification of predictive factors for 3D RFC.

Independent Variables	MRFC (cm)			CRFC (cm)		
	β	<i>p</i>	Adjusted R^2	β	<i>p</i>	Adjusted R^2
Model 1						
Group (vs. 1: TPA < 14°)			0.383			0.384
2: TPA ≥ 14° and KA < 5°	-0.058	0.501		-0.056	0.519	
3: TPA ≥ 14° and KA ≥ 5°	-0.353	0.002		-0.461	<0.001	
FL (cm)	0.295	<0.001		0.295	<0.001	
FOA (°)	-0.328	0.003		-0.213	0.047	
Model 2						
Age (years)	-0.274	0.003	0.354	-0.252	0.008	0.306
FL (cm)	0.228	0.005		0.227	0.007	
KA (°)	-0.386	<0.001		-0.358	<0.001	

Note: Model 1 included sagittal group, gender, age, BMI, FL, C7-SVA, PI-LL, SS, FOA, and AA into the stepwise procedure. Model 2 included gender, age, BMI, FL, C7-SVA, TPA, SS, PT, KA, and AA into the stepwise procedure. *p*-value < 0.05 were consider significant.

Abbreviations: β , standardized partial regression coefficient; CRFC, cortical radius of femoral curvature; FL, femoral length; FOA, femoral obliquity angle; KA, knee flexion angle; MRFC, medullary radius of femoral curvature.

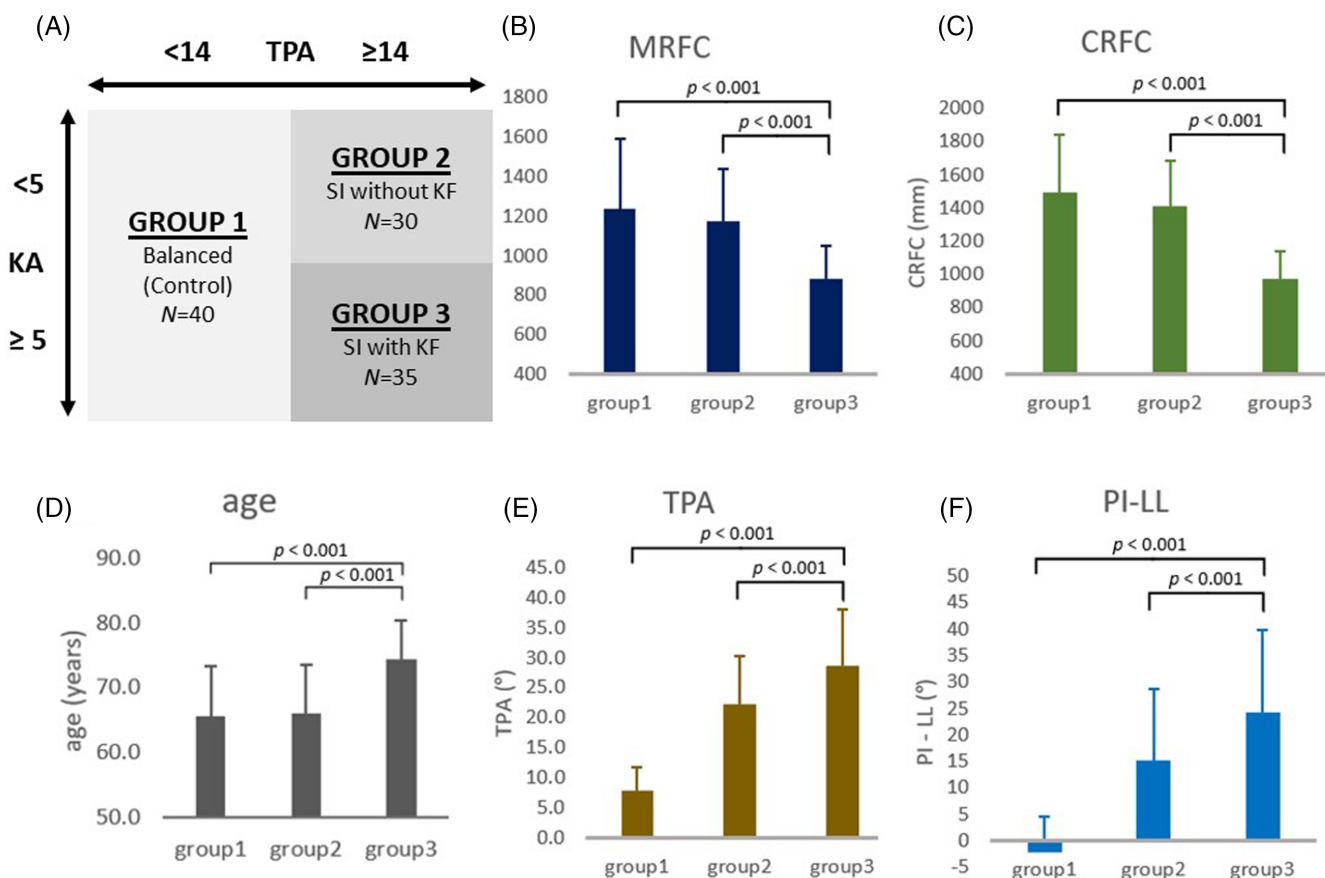


FIGURE 4 Results of subgroup analysis using analysis of covariance with post hoc comparison. The error bars indicate one standard error. (A) Definition of each subgroup: group 1 (N = 40), sagittal balance (control); group 2 (N = 32), SI without KF; group 3 (N = 33), SI with KF. Both (B) medullary RFC and (C) cortical RFC were significantly smaller in group 3 compared to groups 1 and 2. (D) Subjects in group 3 were significantly elder than those in group 1 and 2. (E) Significant difference in TPA was found among subgroups, with group 3 presenting with the greatest TPA and group 1 displaying the smallest. (F) Significant difference in PI-LL, indicating severity of loss of lumbar lordosis, was found among each subgroup, with group 3 presenting with the greatest value and group 1 showing the smallest. CRFC, cortical radius of femoral curvature; FOA, femoral obliquity angle; KA, knee flexion angle; LL, lumbar lordosis; MRFC, medullary radius of femoral curvature; PI, pelvic incidence; TPA, T1-pelvic angle.

4.1 | Associations between femoral curvature and LE CMs

The quantification methods and correlated variables of femoral bowing varied among previous studies. Considering ethnicity, greater bowing was reported in Asian populations compared to Caucasian people.³¹ As for gender, smaller RFC in female femurs was reported.^{5,6} Karakaş and Harma³² reported a decreased RFC in older subjects, yet with a weak correlation. Significant correlation between FL and RFC, with increased RFC in longer femurs, seems to be the most consistent conclusion among previous studies. Maratt et al.⁵ reported similar results of correlation but concluded that significant differences in RFC among gender, height, and ethnicity existed because of the variations in average femoral length between different subgroups based on a regression analysis of large sample size ($n = 3922$). Thiesen et al.⁶ also conducted regression analysis and matched pair subgroup analysis with a relatively large sample size ($n = 1232$), which suggested that FL was the most powerful predictor of femoral bowing followed by age, explaining 22% of variability in RFC. The current study reveals compatible results, but aside from age and FL, implying that parameters of LE CMs including KA and FOA are also associated with 3D RFC. Therefore, the extent of LE CMs were also independent factors in the analysis of femoral bowing of patients with SI.

The results of the present study disclosed that subjects with SI and knee flexion exhibit greater femoral bowing, however, no significant difference in RFC was found between group 1 (sagittal balance) and 2 (SI without knee flexion). In other words, in addition to global imbalance, subjects without flexing their knees to restore postural balance possess RFC similar to that of the healthy population. Furthermore, greater TPA and elder age in group 3 compared to the other two groups are revealed in the present study.

Studies showed that knee flexion is usually the later CMs and is more often recruited in prolonged and severe sagittal malalignment in subjects with severely degenerative spine when spinal and pelvic compensations are inadequate to restore proper postural balance.^{4,33-35} The regional heterogeneity of femoral shaft nature was revealed by previous studies, where posterior region exhibited the highest porosity, smallest density, and lowest stiffness values.³⁶ Zhang et al. discovered that femoral bowing was negatively associated with femoral cortical thickness and significantly increased in the aging process. A hypothesis was proposed in which the regional heterogeneity in cortical bone loss of femoral shaft with aging could lead to the non-uniformity of anteroposterior cortical strength, which further caused an off-centered stress concentration and a substantial morphological change as consequences.³⁷ Considering the greater torque from gravity in patients with SI and flexing knee, it is possible that this additional stress exacerbates the off-center load distribution and leads to increased bowing of the femoral shaft. Based on this hypothesis, the increase in femoral bowing could be a consequence of sagittal malalignment, which should be regarded as one of the LE CMs since it contributes to restoring the center of gravity in individuals with long-term sagittal malalignment. However, due to the limitations of the cross-sectional study design, it is crucial to conduct further longitudinal studies to elucidate this assumption and establish the cause-

and-effect relationship between sagittal malalignment, LE CMs, and femoral bowing.

The clinical impact and potential applications of this study are primarily associated with joint surgeries and femoral implants. The complication rate is lower when using a cephalomedullary nail with a radius of curvature (ROC) of 150 cm compared to a nail with an ROC of 200 cm in the geriatric population.³⁸ However, our data show that the average RFC of patients with SI and KF is less than 100 cm (Figure 4). Consequently, this specific population, which is also at a higher risk of undergoing operations involving femoral implants, might require detailed preoperative evaluations of femoral morphology. Additionally, this study might encourage implant manufacturers to design more curved femoral nails for patients with SI and KF, potentially reducing the risks of surgical complications.

4.2 | Limitations

The present study has several limitations that should be acknowledged. First, the relatively small sample size may limit the generalizability of the statistical results. However, a statistical power analysis was performed, indicating that the sample size was adequate for the major findings of this study. Additionally, despite the sample size, significant results were observed in the statistical analyses conducted. Second, the measurement method used for 3D RFC relied primarily on visual observation. Due to limitations imposed by the EOS imaging system, the computer-aided image editing software used in previous studies was not applicable in this study. Nevertheless, the interobserver and intra-observer reproducibility and precision of the measurement method were assessed using the intraclass correlation coefficient (ICC), demonstrating good reliability of the measurements. Last, this study employed a cross-sectional design, which allows for the analysis of temporal correlations but cannot establish a cause-and-effect relationship. Therefore, a longitudinal study with a larger sample size is necessary to further elucidate and verify the exact effects of sagittal spinopelvic malalignment on femoral bowing.

5 | CONCLUSION

Subjects with SI and flexing knee exhibit greater femoral bowing. Aside from age and FL, two previously reported impact factor of femoral bowing, KA and FOA are as well identified as independent predictive factors of femoral curvature. As a result, orthopedic surgeons should carefully evaluate preoperative radiographs in SI patients undergoing femoral implant surgery. Future research should aim to investigate the causal relationship between sagittal spinopelvic malalignment and femoral bowing through prospective longitudinal studies.

ACKNOWLEDGMENTS

This study was supported by grants funded by the Ministry of Science and Technology, Taiwan (MOST 110-2314-B-006-027-MY3) to Cheng-Li Lin and (MOST 108-2813-C-006-114-B) to Chien-Hsiung

Lo. This study was also supported by National Cheng Kung University Hospital, Tainan, Taiwan (NCKUH-11202056) to Cheng-Li Lin. The authors gratefully acknowledge the Summer Research Project Grant No. NCKUMCS2019040 from College of Medicine at National Cheng Kung University.

CONFLICT OF INTEREST STATEMENT

The authors declare no conflicts of interest.

ORCID

Cheng-Li Lin  <https://orcid.org/0000-0002-7315-7709>

REFERENCES

- Yagi M, Kaneko S, Yato Y, Asazuma T. Standing balance and compensatory mechanisms in patients with adult spinal deformity. *Spine*. 2017;42(10):E584-E591.
- Diebo BG, Ferrero E, Lafage R, et al. Recruitment of compensatory mechanisms in sagittal spinal malalignment is age and regional deformity dependent: a full-standing axis analysis of key radiographical parameters. *Spine*. 2015;40(9):642-649.
- Shimizu T, Cerpa M, Lenke LG. Understanding sagittal compensation in adult spinal deformity patients: relationship between pelvic tilt and lower-extremity position. *J Neurosurg Spine*. 2021;1:1-8.
- Le Huec J, Thompson W, Mohsinaly Y, Barrey C, Faundez A. Sagittal balance of the spine. *Eur Spine J*. 2019;28(9):1889-1905.
- Maratt J, Schilling PL, Holcombe S, et al. Variation in the femoral bow: a novel high-throughput analysis of 3922 femurs on cross-sectional imaging. *J Orthop Trauma*. 2014;28(1):6-9.
- Thiesen DM, Prange F, Berger-Groch J, et al. Femoral anteversion—a 3D CT analysis of 1232 adult femurs. *PLoS One*. 2018;13(10):e0204961.
- Dietrich TJ, Pfirrmann CW, Schwab A, Pankalla K, Buck FM. Comparison of radiation dose, workflow, patient comfort and financial break-even of standard digital radiography and a novel biplanar low-dose X-ray system for upright full-length lower limb and whole spine radiography. *Skeletal Radiol*. 2013;42(7):959-967.
- Melhem E, Assi A, El Rachkidi R, Ghanem I. EOS® biplanar X-ray imaging: concept, developments, benefits, and limitations. *J Child Orthop*. 2016;10(1):1-14.
- Boese CK, Frink M, Jostmeier J, et al. The modified femoral neck-shaft angle: age- and sex-dependent reference values and reliability analysis. *Biomed Res Int*. 2016;2016:1-7.
- Chaibi Y, Cresson T, Aubert B, et al. Fast 3D reconstruction of the lower limb using a parametric model and statistical inferences and clinical measurements calculation from biplanar X-rays. *Comput Methods Biomech Biomed Engin*. 2012;15(5):457-466.
- Chuang H-C, Tseng Y-H, Chen Y, et al. Assessment of sagittal spinopelvic parameters in a Taiwanese population with spondylolysis by the EOS imaging system: a retrospective radiological analysis. *BMC Musculoskelet Disord*. 2021;22(1):1-9.
- Wybier M, Bossard P. Musculoskeletal imaging in progress: the EOS imaging system. *Joint Bone Spine*. 2013;80(3):238-243.
- Amabile C, Le Huec J-C, Skalli W. Invariance of head-pelvis alignment and compensatory mechanisms for asymptomatic adults older than 49 years. *Eur Spine J*. 2018;27(2):458-466.
- Amabile C, Pillet H, Lafage V, Barrey C, Vital J-M, Skalli W. A new quasi-invariant parameter characterizing the postural alignment of young asymptomatic adults. *Eur Spine J*. 2016;25(11):3666-3674.
- Protosaltis T, Schwab F, Bronsard N, et al. The T1 pelvic angle, a novel radiographic measure of global sagittal deformity, accounts for both spinal inclination and pelvic tilt and correlates with health-related quality of life. *J Bone Joint Surg Am*. 2014;96(19):1631-1640.
- Vialle R, Levassor N, Rillardon L, Templier A, Skalli W, Guigui P. Radiographic analysis of the sagittal alignment and balance of the spine in asymptomatic subjects. *J Bone Joint Surg Am*. 2005;87(2):260-267.
- Hasegawa K, Okamoto M, Hatsushikano S, Shimoda H, Ono M, Watanabe K. Normative values of spino-pelvic sagittal alignment, balance, age, and health-related quality of life in a cohort of healthy adult subjects. *Eur Spine J*. 2016;25(11):3675-3686.
- Chantarapanich N, Sitthiseripratip K, Mahaisavariya B, Wongcumchang M, Siribodhi P. 3D Geometrical assessment of femoral curvature: a reverse engineering technique. *J Med Assoc Thai*. 2011;91(9):1377.
- Lu Z-H, Yu J-K, Chen L-X, Gong X, Wang Y-J, Leung KKM. Computed tomographic measurement of gender differences in bowing of the sagittal femoral shaft in persons older than 50 years. *J Arthroplasty*. 2012;27(6):1216-1220.
- Wu J, Wei F, Ma L, et al. Accuracy and reliability of standing lateral lumbar radiographs for measurements of spinopelvic parameters. *Spine*. 2021;46(15):1033-1038.
- Somoskeöy S, Tunyogi-Csapó M, Bogyó C, Illés T. Accuracy and reliability of coronal and sagittal spinal curvature data based on patient-specific three-dimensional models created by the EOS 2D/3D imaging system. *Spine J*. 2012;12(11):1052-1059.
- Guezou-Philippe A, Dardenne G, Dorniol M, Letissier H, Lefèvre C, Stindel E. Reliability of pelvic parameters measurement with sterEOS: preliminary results. *EPIC Series Health Sci*. 2019;3:157-160.
- Koo TK, Li MY. A guideline of selecting and reporting intraclass correlation coefficients for reliability research. *J Chiropr Med*. 2016;15(2):155-163.
- Faul F, Erdfelder E, Lang A-G, Buchner A. G* Power 3: a flexible statistical power analysis program for the social, behavioral, and biomedical sciences. *Behav Res Methods*. 2007;39(2):175-191.
- Su X-Y, Zhao Z, Zhao J-X, et al. Three-dimensional analysis of the curvature of the femoral canal in 426 Chinese femurs. *Biomed Res Int*. 2015;2015:1-8.
- Shackelford LL, Trinkaus E. Late Pleistocene human femoral diaphyseal curvature. *Am J Phys Anthropol*. 2002;118(4):359-370.
- Abdelal AHK, Yamamoto N, Hayashi K, et al. Radiological assessment of the femoral bowing in Japanese population. *SICOT-J*. 2016;2:2.
- Collinge CA, Beltran CMJ. Does modern nail geometry affect positioning in the distal femur of elderly patients with hip fractures? A comparison of otherwise identical intramedullary nails with a 200 versus 150 cm radius of curvature. *J Orthop Trauma*. 2013;27(6):299-302.
- Bazylewicz DB, Egol KA, Koval KJ. Cortical encroachment after cephalomedullary nailing of the proximal femur: evaluation of a more anatomic radius of curvature. *J Orthop Trauma*. 2013;27(6):303-307.
- Park Y-C, Song H-K, Zheng X-L, Yang K-H. Intramedullary nailing for atypical femoral fracture with excessive anterolateral bowing. *J Bone Joint Surg Am*. 2017;99(9):726-735.
- Schmutz B, Kmiec S, Wullschlegel ME, Altmann M, Schuetz M. 3D Computer graphical anatomy study of the femur: a basis for a new nail design. *Arch Orthop Trauma Surg*. 2017;137(3):321-331.
- Karakaş HM, Harma A. Femoral shaft bowing with age: a digital radiological study of Anatolian Caucasian adults. *Diagn Interv Radiol*. 2008;14(1):29-32.
- Obeid I, Hauger O, Aunoble S, Bourghli A, Pellet N, Vital J-M. Global analysis of sagittal spinal alignment in major deformities: correlation between lack of lumbar lordosis and flexion of the knee. *Eur Spine J*. 2011;20(5):681-685.
- Barrey C, Roussouly P, Perrin G, Le Huec J-C. Sagittal balance disorders in severe degenerative spine. Can we identify the compensatory mechanisms? *Eur Spine J*. 2011;20(5):626-633.
- Ferrero E, Liabaud B, Challier V, et al. Role of pelvic translation and lower-extremity compensation to maintain gravity line position in spinal deformity. *J Neurosurg Spine*. 2016;24(3):436-446.
- Rohrbach D, Grimal Q, Varga P, et al. Distribution of mesoscale elastic properties and mass density in the human femoral shaft. *Connect Tissue Res*. 2015;56(2):120-132.

37. Zhang J-Z, Zhao K, Li J-Y, Zhu Y-B, Zhang Y-Z. Age-related dynamic deformation of the femoral shaft and associated osteoporotic factors: a retrospective study in Chinese adults. *Arch Osteoporos*. 2020;15(1):1-7.

SUPPORTING INFORMATION

Additional supporting information can be found online in the Supporting Information section at the end of this article.

How to cite this article: Lo, C.-H., Dean Fang, Y.-H., Wang, J.-Y., Yu, T.-P., Chuang, H.-C., Liu, Y.-F., Chang, C.-J., & Lin, C.-L. (2024). Associations between femoral 3D curvature and sagittal imbalance of spine. *JOR Spine*, 7(1), e1305. <https://doi.org/10.1002/jsp2.1305>